Influence of Butyl Side Chain Elimination, Tail Amine Functional Addition, and C2 Methylation on the Dynamics and Transport Properties of Imidazolium-Based [Tf 2 N −] Ionic Liquid...

ARTICLE *in* JOURNAL OF CHEMICAL & ENGINEERING DATA · JANUARY 2015

Impact Factor: 2.04 · DOI: 10.1021/je500618w

2 AUTHORS:

Mohammad H. Kowsari

Institute for Advanced Studies in Basic Scien...

14 PUBLICATIONS **120** CITATIONS

SEE PROFILE

Mostafa Fakhraee

Sharif University of Technology

6 PUBLICATIONS **7** CITATIONS

SEE PROFILE

Journal of chemical & engineering data

Article

pubs.acs.org/jced

Influence of Butyl Side Chain Elimination, Tail Amine Functional Addition, and C2 Methylation on the Dynamics and Transport Properties of Imidazolium-Based [Tf_2N^-] Ionic Liquids from Molecular Dynamics Simulations

Mohammad H. Kowsari*[,†] and Mostafa Fakhraee[§,‡]

[†]Department of Chemistry and Center for Research in Climate Change and Global Warming (CRCC), Institute for Advanced Studies in Basic Sciences (IASBS), Zanjan 45137-66731, Iran

[‡]Department of Chemistry, Isfahan University of Technology, Isfahan 84156-83111, Iran

ABSTRACT: Molecular dynamics simulations of four ionic liquids (ILs) based on the [Tf_2N]$^-$, bis(trifluoromethanesulfonyl)imide anion, and imidazolium cations with different alkyl side chains have been performed. These simulations investigate the influence of butyl side chain elimination, tail amine functional addition, and C2 methylation on the dynamics and transport properties of this family of ionic liquids at 400 K. In our earlier work (*J. Chem. Eng. Data*, **2014**, 59, 2834−2849), a suite of thermodynamic quantities and microscopic structures of these ILs were studied by classical molecular dynamics simulations and *ab initio* calculations. In this work, the dynamics of the ILs are studied by calculating the mean-square displacement (MSD) and the velocity autocorrelation function (VACF) for selected atomic sites and the centers of mass of the ions. These results are used to calculate the self-diffusion and the ionic conductivity from both the Einstein and Green−Kubo formulas. The calculated ionic self-diffusion coefficients are used to estimate the cationic transference number and the Stokes−Einstein viscosity for the four ILs. In agreement with experiments, the general simulated trends in the MSD, self-diffusion, and ionic conductivity are [bmim][Tf_2N] > [apmim][Tf_2N] > [bmmim][Tf_2N] > [mim][Tf_2N]. These trends are the reverse of the trend in the viscosity of four selected ILs. As expected by applying a nonpolarizable force field, the simulation results tend to underestimate the self-diffusivity and conductivity, and overestimate the shear viscosity. The highest and the lowest degrees of ionic association are detected for [mim][Tf_2N] and [bmim][Tf_2N], respectively.

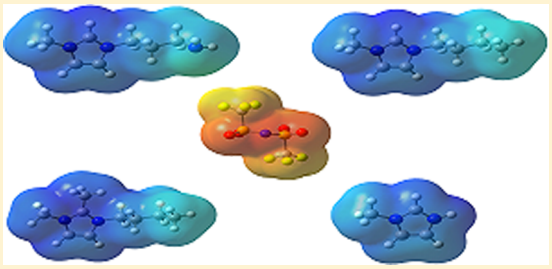

1. INTRODUCTION

Room temperature ionic liquids (RTILs) are generally composed of an asymmetric and large organic cation (based on imidazolium, pyrrolidinium, ammonium, phosphonium, guanidinium, pyridinium, or other cations) and an inorganic anion (halides, nitrate, tetrafluoroborate, hexafluorophosphate, triflate and bis-triflimide or other large, charge-diffuse anions).[1−5] These salts have many applications in synthesis,[6,7] catalysis,[6,8] separation,[1,9] extraction,[3,10,11] and lubrication.[1,9] Academic and industrial investigations on the ILs have increased owing to their special properties such as non-flammability, negligible vapor pressure at room temperature, low melting point, high thermal stability, wide electrochemical window, capability to operate as successful solvents for numerous reactions, and also capability to dissolve a variety of polar or nonpolar, organic and inorganic compounds.[5,12−16] Various physical and chemical properties of ILs depend on the cation and anion,[2,16,17] and simulations can provide systematic molecular level understanding of the properties of these neoteric solvents to assist experimentalists in the design and synthesis of new ILs suitable for specific applications.

Ionic liquids based on 1-alkyl-3-methylimidazolium cations with the bis(trifluoromethanesulfonyl)imide anion, that is, the ([$C_n$mim][Tf_2N]) family, have recently attracted attention. These ILs have a relatively low viscosity, high thermal, electrochemical, and moisture stability, and the unique solution properties in the experimental applications.[2] The strong delocalization and diffuse nature of the negative charge in the S−N−S core of [Tf_2N]$^-$ leads to a reduction in cation−anion interactions.

The experimental measurement of transport properties of ILs is difficult because of the high sensitivity to impurities such as water and halide ions on the measured properties. This shows the advantage of atomistic molecular dynamics as a tool in the prediction of the aforementioned properties.

In this work, molecular dynamics (MD) simulations are used to study the translational dynamics and transport properties of four ILs consisting of imidazolium-based cations with different combinations of alkyl side chains (namely, [bmmim]$^+$, 1-butyl-2,3-dimethylimidazolium; [bmim]$^+$, 1-butyl-3-methylimidazolium; [apmim]$^+$, 1-(3-aminopropyl)-3-methylimidazolium; [mim]$^+$, 1-methyl-imidazolium), and the weakly coordinating

Received: July 2, 2014
Accepted: December 22, 2014

DOI: 10.1021/je500618w
J. Chem. Eng. Data XXXX, XXX, XXX−XXX

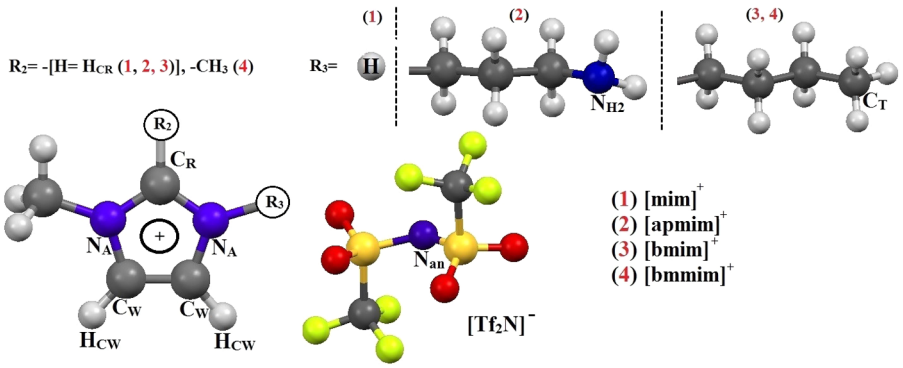

Figure 1. Four imidazolium cations and the $[Tf_2N]^-$ with the main atomic labels according to the applied force fields in this study.

anion $[Tf_2N]^-$, see Figure 1. There are numerous studies available in the literature on experimental and theoretical determined transport properties of [bmim][Tf_2N]. Among the four selected ILs in this work, transport properties of [bmim][Tf_2N] are used as a benchmark to evaluate the current simulation results. To the authors' knowledge, this is the first study of the transport properties of the [mim][Tf_2N] IL. In addition, examination of transport properties of the amine-functionalized task-specific [apmim][Tf_2N] and a comparison with properties of [bmim][Tf_2N] will clarify the influences of amine addition on the properties of ILs. There are a limited number of MD studies on amine-functionalized ILs.[18−20] The current is the second MD simulation of transport properties of [apmim][Tf_2N] after the work of Gutowski and Maginn.[19]

In addition we focus on detailed descriptions of the influences of C2 methylation or converting 1-*n*-butyl side chain of $[bmim]^+$ to hydrogen or 1-(3-aminopropyl), resulting in $[mim]^+$ and $[apmim]^+$ cations, respectively, on the dynamics and transport properties of four imidazolium-based $[Tf_2N^-]$ ILs.

This work is organized as follows: in section 2 simulation details are reported. In section 3 the methodology applied to calculate the dynamics and transport properties of four ILs, and the results of the MD simulations are presented and discussed. Summary and conclusions are given in section 4.

2. MD SIMULATION DETAILS

The force field parameters used in the MD simulations for $[bmmim]^+$, $[bmim]^+$, $[mim]^+$, and $[Tf_2N]^-$ ions are taken from the systematic all-atom force field of Canongia Lopes et al.,[21−23] and the force field used for $[apmim]^+$ was developed by Gutowski and Maginn.[19] The applied total potential energy has the following standard functional form:

$$V_{tot} = \sum_{bonds} k_b(r - r_{eq})^2 + \sum_{angles} k_\theta(\theta - \theta_{eq})^2 + \sum_{dihedrals} k_\phi[1 + \cos(n\phi - \delta)] + \sum_{i=1}^{N-1}\sum_{j>1}^{N}\left\{4\varepsilon_{ij}\left[\left(\frac{\sigma_{ij}}{r_{ij}}\right)^{12} - \left(\frac{\sigma_{ij}}{r_{ij}}\right)^{6}\right] + \frac{q_i q_j}{4\pi\varepsilon_0 r_{ij}}\right\} \quad (1)$$

This force field contains intramolecular (bonds, angles and torsional dihedral interactions) and intermolecular potential terms. The latter terms are described by the pairwise additive atom−atom 12−6 Lennard-Jones potential for van der Waals interactions and Coulombic point changes for electrostatic interactions. Further details of the force field are given in our earlier work[24] and are not repeated here. All simulations are performed on systems consisting of 125 to 180 ion pairs using the DL_POLY 2.18 program,[25] with a time step of 1 fs with the Verlet leapfrog algorithm. The electrostatic long-range interactions were treated using the Ewald summation method with a precision of 10^{-6} and short-range interactions were considered below the cutoff distance of 16.5 Å. Simulations were done in the *NpT* Nosé−Hoover[26,27] barostat−thermostat algorithm. Procedural details for equilibrating the system were given in our earlier work.[24] To calculate dynamic properties such as the mean-square displacement (MSD) and transport coefficients from the Einstein relations, each of the equilibrated systems was studied with a long 7.5 ns *NpT* simulation at 400 K. The velocity and electric current autocorrelation functions were obtained by averaging results from the eight short *NpT* runs each of 55 ps length. The initial configuration of these short runs was taken from the end configuration of the long (7.5 ns) simulation.

3. RESULTS AND DISCUSSION

3.1. Dynamic Properties and Self-Diffusion. To study the microscopic motion of the ions and to quantify the liquid dynamics in detail, we calculate the normalized velocity autocorrelation function (VACF), $C_{vv}(t)$, and the MSD for the centers of mass of the ions from MD simulations. The normalized VACF is defined as

$$C_{vv}(t) = \frac{1}{N}\sum_{i=1}^{N}\frac{\langle \mathbf{v}_i^{com}(t)\cdot\mathbf{v}_i^{com}(0)\rangle}{\langle \mathbf{v}_i^{com}(0)\cdot\mathbf{v}_i^{com}(0)\rangle} \quad (2)$$

where N is the number of ions i in the system and $\mathbf{v}_i^{com}(t)$ is the velocity (vector) of the center of mass of the ion and the brackets $\langle\rangle$ represent an ensemble average over all time origins. The normalized VACF is related to the self-diffusion coefficient of ion i using the Green−Kubo integral formula,[28]

$$D = \frac{k_B T}{m}\int_0^\infty C_{vv}(t)\,dt \quad (3)$$

where k_B is the Boltzmann constant and m is the ionic mass.

The MSD is defined as[16,28,29]

$$MSD(t) = \frac{1}{N}\sum_{i=1}^{N}\langle[\mathbf{r}_i^{com}(t) - \mathbf{r}_i^{com}(0)]^2\rangle \quad (4)$$

where $[\mathbf{r}_i^{com}(t) - \mathbf{r}_i^{com}(0)]$ is the (vector) distance traveled by the center of mass of ion i over some time interval t, and the squared magnitude of this vector is averaged (as indicated by

DOI: 10.1021/je500618w
J. Chem. Eng. Data XXXX, XXX, XXX−XXX

the angle brackets) over many such time intervals. This quantity is averaged also over all cations or anions (N) in the system for improved statistical precision. The self-diffusion coefficient can also be calculated from the long-time limit of the center of mass MSD by the widely used Einstein relation

$$D = \frac{1}{6}\lim_{t\to\infty}\frac{d}{dt}[\mathrm{MSD}(t)] \quad (5)$$

Ionic transference numbers (t_i) help to understand the relative contributions of the anion and cation to the transfer of the total charge in the ionic liquids when they are used in electrolyte applications.[29] The ionic transference numbers for the monovalent ions $[im]^+$ and $[Tf_2N]^-$, may be estimated from the diffusion coefficients of the cation and anion, $t_+ = D_+/(D_+ + D_-)$ and $t_- = D_-/(D_+ + D_-)$, where, $t_+ + t_- = 1$ and $0 \le t_i \le 1$.

The normalized center of mass VACFs of partner cations and anions of the four ILs from trajectory averaging of eight short NpT simulations at 400 K are plotted in Figure 2. The

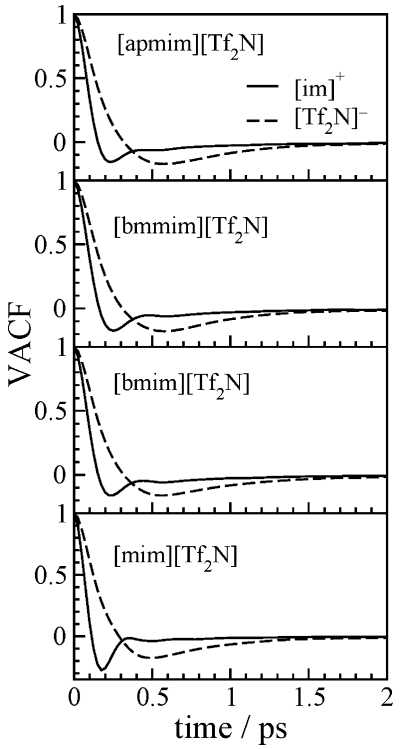

Figure 2. Computed normalized center of mass VACFs of the four imidazolium cations (solid lines) and partner $[Tf_2N]^-$ (dashed lines) of four ionic liquids at 400 K.

influences of the alkyl side chain in the cations or ionic mass on the computed VACFs can be observed in Figure 3. In each ionic liquid, the short-time translational dynamic behavior of the imidazolium cation and the associated $[Tf_2N]^-$ differ from one another. The time scales of the VACFs decay are shorter for the cations than the $[Tf_2N]^-$ anions. The first zero in the VACFs, which is an approximate measure of a mean collision time for each ion, is observed to be 0.11 ps for $[mim]^+$, 0.16 ps for the other three imidazolium cations, and 0.32 ps for $[Tf_2N]^-$ anions. The molar mass of the $[Tf_2N]^-$ (280.15 g·mol^{-1}) is around twice that of the molar mass of $[apmim]^+$, $[bmim]^+$, and $[bmmim]^+$ cations and higher than three times that of $[mim]^+$ (83.11 g·mol^{-1}). Thus, the ionic mass can be a factor determining the short-time relative pattern of the VACF

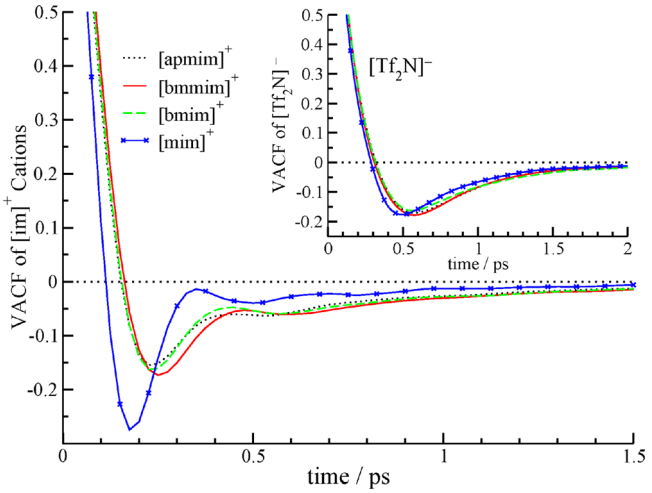

Figure 3. Normalized VACFs of imidazolium cations of four [im][Tf_2N] ILs at 400 K. In the inset, the normalized VACFs of four partner $[Tf_2N]^-$ anions are shown for comparison.

of counterions in ILs. After the first collision of a given ion with a nearest neighbor, the direction of its velocity vector, $\mathbf{v}_i^{com}(t)$, is partially reversed compared to its initial reference velocity, $\mathbf{v}_i^{com}(0)$, and the VACF shows a negative region. Continuous collisions with neighbors results in eliminating velocity correlations at a time (the "second zero time") in the range of 0.37 ps to 1 ps for the lightest ion, $[mim]^+$, 0.57 ps to 1.5 ps for other cations $[apmim]^+$, $[bmim]^+$, and $[bmmim]^+$ and 1.5 ps to 2 ps for the heavy $[Tf_2N]^-$ as shown in Figures 2 and 3.

The MSDs for the ion center of mass and selected atomic sites of the cations and anions in [apmim][Tf_2N] and [bmim][Tf_2N] ILs from the 7.5 ns simulations at 400 K are shown in Figure 4. The MSDs for the nitrogen atom (NH_2) of the amine group on $[apmim]^+$ or the terminal carbon atom (C_T) in the butyl side chain of $[bmim]^+$ are significantly higher

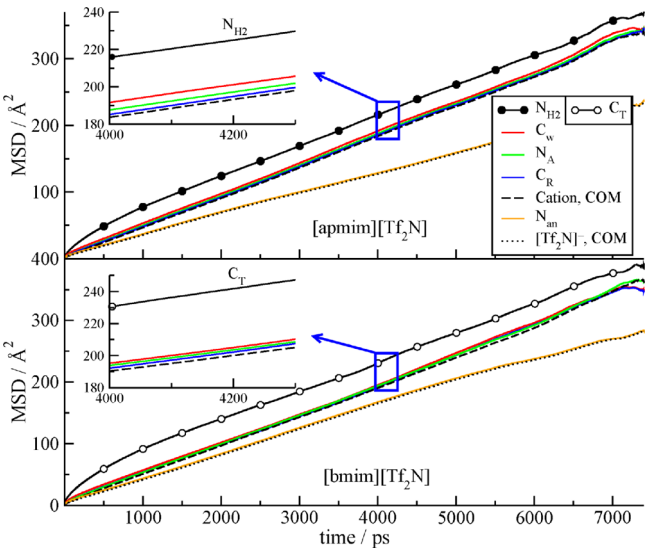

Figure 4. Calculated MSDs for ionic center of mass (COM) and selected atomic sites of imidazolium cations and $[Tf_2N]^-$ in [apmim][Tf_2N] and [bmim][Tf_2N] ILs at 400 K. The insets show the magnified MSD behavior of atomic sites of imidazolium cations in the time range of 4000 ps to 4300 ps. The atomic labels are shown in Figure 1.

DOI: 10.1021/je500618w
J. Chem. Eng. Data XXXX, XXX, XXX−XXX

than those of atoms in the imidazolium ring (N_A, C_w, and C_R, shown in Figure 1). This suggests greater flexibility of the side chain and maybe weaker interactions between the chains. As shown in Figure 4, the MSDs of the central carbon atom (C_R or C2) or the nitrogen (N_A) of imidazolium ring and the nitrogen atom (N_{an}) of $[Tf_2N]^-$ are equal with the cation and anion center of mass. This is to be expected based on the ionic structure.

The MSD of the center of mass of cations and anions of four ILs from *NpT* simulations performed up to a time of ~7.5 ns are shown in Figure 5. In agreement with the experiment for

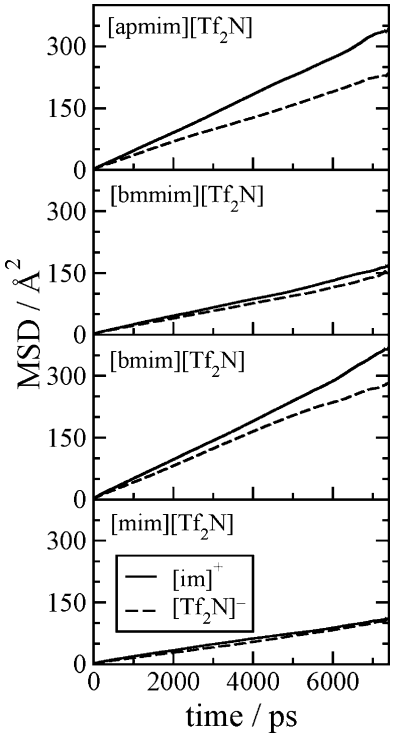

Figure 5. Computed center of mass MSDs of imidazolium cations (solid lines) and partner $[Tf_2N]^-$ anions (dashed lines) of four ionic liquids from *NpT* simulations at 400 K up to a time of ~7.5 ns. For all systems, in agreement with experiment, the MSD of the imidazolium cation is higher than the MSD of the $[Tf_2N]^-$.

each ionic liquid, the MSD of the imidazolium cation is larger than that of the $[Tf_2N]^-$. However, in general, the MSDs and the diffusion coefficients are close in magnitude for the cation and its partner $[Tf_2N]^-$ in each panel, especially for the [bmmim][Tf_2N] and [mim][Tf_2N] cases.

The influence of the alkyl/functional side chain of the four imidazolium cations on the computed MSDs are shown in Figure 6. The magnitude of the MSD at each times for imidazolium cations is $[bmim]^+ \geq [apmim]^+ > [bmmim]^+ > [mim]^+$. A similar trend holds for the MSDs of the $[Tf_2N]^-$ anions in the different ILs, $[Tf_2N]^-_{([bmim])} > [Tf_2N]^-_{([apmim])} > [Tf_2N]^-_{([bmmim])} > [Tf_2N]^-_{([mim])}$.

The strength of van der Waals (vdW) and electrostatic (Coulombic) interactions between the cations and anions determines the ionic character, diffusion coefficients, and viscosity in each series of ILs. The molar values of the E_{vdW}, E_{Coul}, and the intermolecular energy, E_{inter}, ($E_{inter} = E_{vdW} + E_{Coul}$) calculated at 400 K are given in Table 1. For each ionic liquid, $|E_{Coul}| > |E_{vdW}|$, which shows electrostatic interactions are

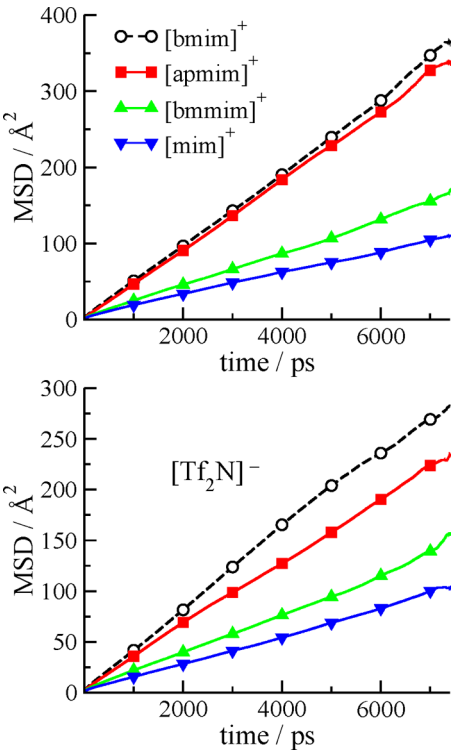

Figure 6. Calculated center of mass MSDs of four imidazolium cations (upper panel) and their partner $[Tf_2N]^-$ anions (lower panel) of ionic liquids from *NpT* simulations at 400 K.

more dominant in these ILs. As expected, the magnitude of E_{vdW} increases with an increase in the number of atoms in the imidazolium cation: [bmmim][Tf_2N] > [bmim][Tf_2N] > [apmim][Tf_2N] > [mim][Tf_2N], while, the calculated trends for E_{Coul} and E_{inter} of ILs are [apmim][Tf_2N] > [mim][Tf_2N] > [bmmim][Tf_2N] > [bmim][Tf_2N]. Except for that of [apmim]-[Tf_2N], the order of E_{Coul} is opposite that of the observed MSD trend. As seen in Table 1, the magnitudes of E_{Coul} and E_{inter} for [apmim][Tf_2N] are different from those of the other ILs. This IL is simulated with a different cation force field which applied relatively larger values of point charges on the atom sites of $[apmim]^+$ in comparison with similar sites for the other three imidazolium-based cations.

As shown in Figure 6, the cation and anion in [mim][Tf_2N] both have the lowest values of MSD in comparison with the corresponding ions in the three others ILs of this study. This is related to the better packing of the ions in [mim][Tf_2N],[24] and the relatively lower charge delocalization in $[mim]^+$ which leads to stronger ion association. The stronger ion association in this IL is in good agreement with the previously determined results of calculated density, cation−anion distance from optimized structure of the ion pair, and cation−cation and anion−anion radial distribution function (RDF) analysis, see Figures 2 and 4 in our earlier work.[24] Figure 6 shows that the C2 methylated $[bmmim]^+$ and amine ($-NH_2$) functionalized $[apmim]^+$ cations have lower MSD and translational motion compared to $[bmim]^+$.

In Table 2, we summarize the calculated ionic diffusion coefficients of the four simulated ILs from both the MSD and VACF methods. Recent experience[16,19,30,31] shows that because of the generally slow dynamics and high viscosity of ILs, long MD trajectories (between 5 ns and 20 ns) are needed to obtain a reliable value of the Einstein self-diffusion coefficient from the

DOI: 10.1021/je500618w
J. Chem. Eng. Data XXXX, XXX, XXX−XXX

Table 1. Computed van der Waals, E_{vdW}, Electrostatic, E_{Coul}, and Intermolecular, E_{inter}, Energies of the Four ILs at 400 K

ILs	E_{vdW} / kJ·mol^{-1}	E_{Coul} / kJ·mol^{-1}	E_{inter} / kJ·mol^{-1}
[bmmim][Tf_2N]	−113.41 ± 1.23	−142.45 ± 1.64	−255.86 ± 3.09
[bmim][Tf_2N]	−111.50 ± 1.20	−126.28 ± 1.66	−237.78 ± 3.11
[apmim][Tf_2N]	−98.90 ± 1.08	−287.75 ± 1.67	−386.65 ± 3.02
[mim][Tf_2N]	−92.13 ± 0.94	−172.44 ± 1.59	−264.57 ± 2.68

Table 2. Self-Diffusion Coefficient (10^{-11} m^2 s^{-1}) for the Cations and Anions from the Slope of MSD Plots (with β Values in Parentheses) and Integration of the VACFs (with the Subscript Standard Deviations in Parentheses) and the Cationic Transference Number t_+, for Four Ionic Liquids

		MSD			VACF		
ILs	T/K	$D_+(\beta)$	$D_-(\beta)$	t_+	D_+	D_-	t_+
[apmim][Tf_2N]	298				$0.77_{(0.4)}$	$0.62_{(0.4)}$	0.554
	298	0.865[a]	0.620[a]				
[apmim][Tf_2N]	400	7.79 (1.03)	4.78 (0.87)	0.619	$10.97_{(0.8)}$	$8.94_{(0.8)}$	0.551
[bmmim][Tf_2N]	400	3.36 (0.92)	3.04 (0.95)	0.525	$7.93_{(1.1)}$	$6.42_{(1.5)}$	0.553
	393	12.4[b], 17.83[c], 26.8[d]	8.7[b], 12.90[c], 23.3[d]				
[bmim][Tf_2N]	400	7.85 (0.97)	7.02 (0.97)	0.528	$11.99_{(1.2)}$	$10.18_{(1.2)}$	0.541
	400	4.3[e], 9.7[f], 23.1[g], 31.7[d]	3.3[e], 7.3[f], 16.5[g], 23.5[d]		24.48[g]	17.0[g]	
[mim][Tf_2N]	400	2.30 (0.87)	2.23 (0.97)	0.508	$8.19_{(0.8)}$	$7.10_{(0.7)}$	0.536

[a]Reference 19. [b]Reference 42, using a nonpolarizable force field at 393 K. [c]Reference 38, using a nonpolarizable force field at 400 K. [d]Reference 43, using a polarizable force field at 393 K. [e]Reference 32, simulation at 403 K. [f]Reference 44, using the Lopes force field (refs 22 and 23) at 400 K. [g]Reference 33.

slope of the MSD, eq 5. Gabl et al.[31] mentioned at least 500 ion pairs were needed for the correct modeling of the dynamics of ILs; however, many papers successfully report transport properties of ILs for systems consisting of 100+ ion pairs in the simulation box, and we believe it is possible get proper transport properties with similar system size by properly equilibrating the systems. After several extensive equilibration stages for simulation cells containing 125 to 180 ion pairs, we ran ∼7.5 ns NpT simulation trajectories for each ionic liquid, and the ionic self-diffusion coefficient was computed from the linear fitting of the slope of MSD(t) function using data in the range of 2 ns to 5 ns. As reported in Table 2, the calculated values of $\beta(t) = (\mathrm{d}\log \mathrm{MSD}(t))/(\mathrm{d}\log t)$ in this time range for all cases at 400 K are generally ∼1. As linear diffusive behavior corresponds with $\beta = 1$, computing the slope of the MSD(t) function from a linear fitting between 2 ns and 5 ns can give a reasonable estimation of the self-diffusion coefficient at 400 K. Alternatively, the Green−Kubo integral of the VACFs, eq 3, from trajectory-averaging of eight short (∼55 ps) runs was employed to determine the diffusion coefficients for each ion. The integral of the VACFs was evaluated with an upper time limit between 10 ps and 25 ps, and the resulting values were averaged.

The ionic diffusion coefficient in ILs is controlled by the ionic size, ion shape, and the strength of interaction between ions.[16,32] Both the Green−Kubo and Einstein methods show that in all cases, the imidazolium cations have a greater self-diffusivities than the $[Tf_2N]^-$ anions. A similar observation for the relative self-diffusion of the anion and cation in ILs has been reported many times experimentally and computationally.[33] In addition to the lower mass of four imidazolium cations compared to the $[Tf_2N]^-$, preferential translational motion of the imidazolium cation along the plane of the ring, which is analyzed for [bmim][Tf_2N] in detail by Liu and Maginn, leads to greater self-diffusivities of the cations.[33] It can be expected that $N_{H2}\cdots N_{H2}$ and $N_{H2}\cdots H_{CR}$ intermolecular interactions (shown in our earlier work[24]) are the reason for the smaller cation motion in [apmim][Tf_2N] than in [bmim][Tf_2N].

All calculated cationic transference numbers (t_+) are higher than 0.5, reflecting greater diffusivities of planar imidazolium cations. In the experimental cases studied in refs 34 and 35, and also in the recent simulation results of [bmim][Tf_2N] reported by Liu and Maginn,[33] the activation energies for the anion diffusion are higher than that of the cations.

The data in Table 2 show that for the imidazolium cations, the numerical values of ionic self-diffusion coefficients vary in the order of [bmim][Tf_2N] ≥ [apmim][Tf_2N] > [bmmim]-[Tf_2N] > [mim][Tf_2N]. However, the relative magnitude of the diffusion coefficients and other transport properties in ILs are very sensitive to the type of applied force field (especially the set of partial charges employed in the force field[36]) and the temperature of the simulations.[37] Thus, some relative numerical differences in the calculated dynamic properties for [apmim]-[Tf_2N] compared to the three other ILs may be related to the different applied force field source for $[apmim]^+$, see section 2 (simulation details). In addition to the type of force field, due to differences in other simulation conditions, such as equilibration times, overall simulation time, quality of the equilibration, and the time length of production runs, and the method for calculating diffusion coefficients (using the MSD or VACF), the direct comparison of our computed diffusion coefficients with simulations from other computational studies is difficult.

The absolute values of the self-diffusion coefficients from both the MSDs and VACFs in Table 2 are numerically lower than experimental values. However, the Green−Kubo VACF integral method yields higher self-diffusion coefficients than the Einstein MSD approach, and are in better agreement with recent experimental studies.[16,36−40] The fact that $\beta \leq 1$ within the 2 ns to 5 ns time range is used to determine the slope of the MSD may be one of the reasons the diffusion coefficients

DOI: 10.1021/je500618w
J. Chem. Eng. Data XXXX, XXX, XXX−XXX

Table 3. Ionic Conductivity from the Nernst−Einstein Relation, σ_{NE} (10^{-3} S·cm^{-1}), from the Green−Kubo Relation, σ_{GK} (10^{-3} S·cm^{-1}), and the Viscosity from the Stokes−Einstein Relation, η_{SE} (mPa·s), for the Four Ionic Liquids at 400 K

	$\sigma_{NE}/10^{-3}$ (S cm^{-1})			η_{SE}/(mPa s)[a]	
ILs	MSD	VACF	σ_{GK}	MSD	VACF
[apmim][Tf_2N]	12.60	19.88	13.54	28.2	15.08
[bmmim][Tf_2N][b]	5.76	12.93	8.70	44.35	21
[bmim][Tf_2N][c]	14.21 (28.5)	21.27 (29.8)	18.94 (15.5)	19.20 (∼14.2)	13.24 (∼14.2)
[mim][Tf_2N]	5.78	19.50	9.90	60.45	18.99

[a]The effective hydrodynamic (Stokes) radius, r_s, for[Tf_2N]$^-$ (0.326 nm),[58] the anion diffusion coefficient, and c = 4 are used to calculate the viscosity. [b]The calculated Green−Kubo viscosity and ionic conductivity of [bmmim][Tf_2N] at 400 K are 23.12 mPa·s[38] and ∼17.8·10^{-3} S·cm^{-1},[48] respectively. [c]The simulation data in parentheses are from the ref 33. The experimental viscosity and ionic conductivity of [bmim][Tf_2N] at 400 K from extrapolate of the VFT equations are 4.28 mPa·s and 33.74·10^{-3}S·cm^{-1},[34] the calculated η_{GK} for [bmim][Tf_2N] at 400 K is 14.2[33] and 40 mPa·s.[44]

determined from the MSDs are smaller than those calculated from integration of the VACFs.[41]

3.2. Electric-Current Autocorrelation Functions, Ionic Conductivity, and Viscosity. The ionic conductivity, viscosity and self-diffusivity play important roles in many practical applications of ILs in chemistry and chemical engineering. The Nernst−Einstein equation (eq 6) can usually be used for the approximate calculation of the ionic conductivity from the summation of cationic and anionic self-diffusion coefficients,[28,41]

$$\sigma_{NE} = \frac{N_{pair}e^2}{Vk_BT}(q_+^2D_+ + q_-^2D_-) \tag{6}$$

where $q_\pm^2$ = 1 for 1:1 salts, e is the electric charge unit, 1.60219·10^{-19} C, V is the volume of simulation box, and N_{pair} is the number of ion pairs in the simulation. The acceptable accuracy of the Nernst−Einstein equation for predicting the ionic conductivity of imidazolium-based ionic liquids was investigated in previous studies.[16,39,45−48] The Green−Kubo time integral of electric-current autocorrelation function, σ_{GK}, includes the rigorous effects of ionic associations,[28,49]

$$\sigma_{GK} = \frac{1}{3k_BTV}\int_0^\infty \langle \mathbf{j}(t)\cdot\mathbf{j}(0)\rangle \, dt = \sigma_{NE}[1 - \Delta(t)] \tag{7}$$

where the electric-current flux $\mathbf{j}(t) = \sum_{i=1}^{N} q_i\mathbf{v}_i^{com}(t)$, and q_i represents the charge of ion i. The positive parameter $\Delta(t)$, extensively studied by Harris et al.,[51] is related to differences in cross-correlations of ionic velocities. We mentioned previously[16,47] that the $\Delta(t)$ term measures the deviation from the ideal Nernst−Einstein behavior and is directly related to the magnitude of interionic interactions.[47] The electric-current autocorrelation function (ECACF), $J(t)$ can be explicitly defined as[51]

$$\begin{aligned} J(t) &= \langle \mathbf{j}(t)\cdot\mathbf{j}(0)\rangle \\ &= \sum_{i=1}^{N}\sum_{j=1}^{N}\langle q_iq_j\mathbf{v}_i^{com}(t).\,\mathbf{v}_j^{com}(0)\rangle \\ &= Z(t) + \sum_{i=1}^{N}\sum_{j\neq i}^{N}\langle q_iq_j\mathbf{v}_i^{com}(t).\,\mathbf{v}_j^{com}(t)\rangle \\ &= Z(t) + \Delta(t) \end{aligned} \tag{8}$$

in the summation of eq 8, $N = N_{cat} + N_{an}$. In eq 8, $Z(t)$ is a self-term, which is specified as the total velocity autocorrelation function. The cross terms $\Delta(t) = J(t) - Z(t)$, represent ion-pair formation and the deviation from the ideal Nernst−Einstein behavior.

In this study, the ionic conductivity from both the simple Nernst−Einstein, eq 6, and the rigorous Green−Kubo, eq 7, formulas were calculated for the four simulated ILs at 400 K (see Table 3). The calculated ionic conductivities from both methods show the same trends with numerical values on the order of 10^{-3} S cm^{-1} to 10^{-2} S cm^{-1}. This order of magnitude is consistent with other computational and experimental studies of imidazolium salts.[35,37,47,50] The self-diffusion coefficients reported in Table 2 from the Einstein (MSD) relation, eq 5, and from the VACF integral, eq 3, were used to calculate the σ_{NE}. The ionic conductivity values from the VACF diffusion coefficients are in better agreement with the limited available experimental evidence.

After computing the average electric-current autocorrelation functions, $J(t)$, with the ensemble-averaging technique from eight 55 ps runs in the NpT ensemble, we calculated the σ_{GK} by integrating the ECACF with upper time limits in the interval between 10 ps and 25 ps. The general appearance of the ECACF and its time integral for four imidazolium based [Tf_2N^-] ILs is shown in Figure 7.

The effects of the alkyl/functional substituent group in the imidazolium cations on the computed ionic conductivities of these ILs can be also observed (see Table 3). Our conductivity results show the trend of σ[bmim][Tf_2N] > σ[apmim][Tf_2N] > σ[mim][Tf_2N] > σ[bmmim][Tf_2N]. The [apmim][Tf_2N] ionic liquid with the polar −NH_2 functional group in the side chain of the imidazolium cation has a smaller ionic conductivity than [bmim][Tf_2N]. The C2 methylated ionic liquid, [bmmim][Tf_2N], has the lowest ionic conductivity of the group, in agreement with high viscosity and slow dynamics observed for C2 methylated ILs from experimental and computational results.[52−55] [mim]$^+$ is better packed in the liquid phase which can enhance ion-pair association, limiting the motion of [mim]$^+$ (see Figure 6), and this causes relatively low ionic conductivity for this IL. The alkyl chains on the imidazolium cation have different effects on the ionic conductivity of the ILs. [bmim]$^+$ has a smaller surface electrical charge density than [mim]$^+$, and thus the former has higher ionic mobility. However, increasing the alkyl chain length in the 1-alkyl-3-methylimidazolium, [amim]$^+$, may limit the dynamical movement of the cation and decrease its ionic conductivity.[47]

The Nernst−Einstein equation assumes no ionic association between ions in an IL. Comparing the Green−Kubo ionic conductivities with the corresponding ideal Nernst−Einstein values from VACF diffusion coefficients (with similar numerical uncertainties) some details about of the degree of ionic

DOI: 10.1021/je500618w
J. Chem. Eng. Data XXXX, XXX, XXX−XXX

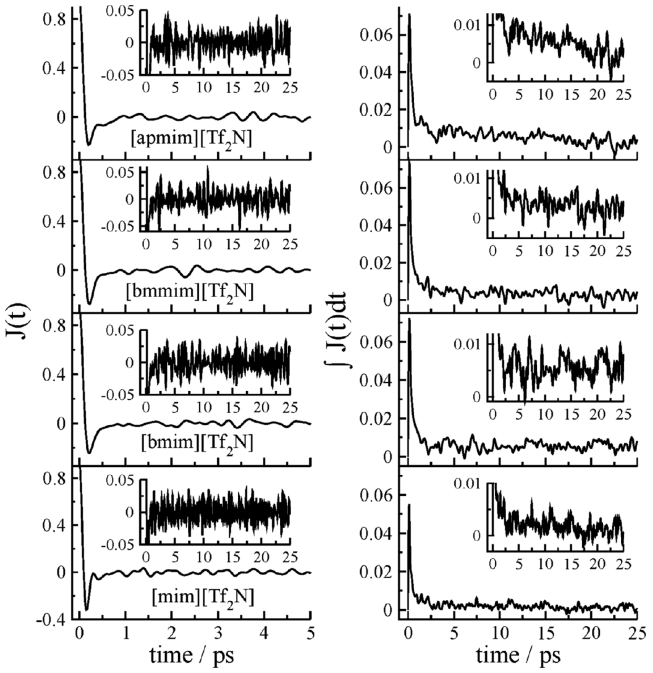

Figure 7. Computed normalized electric-current autocorrelation functions (left). The integration of the electric-current autocorrelation functions of ILs (right). The insets show the magnified long-time behavior of the $J(t)$ and its integral.

association between ions in the studied ILs become obvious. As expected for all four studied cases in Table 3, $\sigma_{GK} < \sigma_{NE}^{(VACF)}$, and the ratio $Y = \sigma_{GK}/\sigma_{NE}^{(VACF)}$ is 0.89, 0.68, 0.67, and 0.51 for [bmim], [apmim], [bmmim], and [mim]-based $[Tf_2N^-]$ ionic liquids, respectively. The Y ratio shows the degree of uncorrelated ion motion or "ionicity"[56,57] in each of the target ionic liquids. When $Y = 1$ ion motion is completely uncorrelated, while when $Y = 0$ ion motions are totally correlated such that anions and cations move in unison.[33] The largest Y ratio is for $[bmim][Tf_2N]$ and shows the lowest ionic association and short-lived ion pairs in $[bmim][Tf_2N]$ compared to the other studied cases. The smaller Y value obtained for $[mim][Tf_2N]$ shows the highest correlated ionic motion in this IL.

The viscosity, η, is a major input for simulation and optimization of processes in engineering design and analysis. The diffusion coefficient is often used to estimate the values of the viscosity by the Stokes–Einstein equation,[16]

$$D = \frac{k_B T}{c\pi\eta r_{s,i}} \tag{9}$$

where c is a constant, and $r_{s,i}$ is the effective hydrodynamic (Stokes) radius of the ion i. The $r_{s,i}$ values for the 1-alkyl-3-methylimidzolium ($[amim]^+$) and $[Tf_2N]^-$ ions have been obtained from the MM2 and *ab initio* molecular orbital calculations on the basis that the ionic van der Waals volume is only determined by the sum of van der Waals radii of atoms.[58] The value of c depends on the nature of the system and the interactions experienced by the solute. The factor c may help to characterize the microscopic ion dynamics in the RTILs.

Tokuda et al.[34,35] have shown a good linear relationship between D_i and $T\eta^{-1}$ for the cationic diffusion coefficients in $[amim][(CF_3SO_2)_2N]$ and [bmim][X] with all lines passing through the origin. This indicates that the viscosity of the solution is the predominant factor in determining the diffusion of the ions in ILs. However, recent studies use the fractional Stokes–Einstein relation, $D_i \propto (T/\eta)^{\beta}$ with $\beta \approx 0.8$ to 0.9.[59−62] In our calculations, we estimate the viscosity using the Stokes–Einstein relation based on the $[Tf_2N]^-$ diffusion coefficients and $c = 4$ for all cases[47] (see Table 3).

The trend in the viscosity in the series of ILs are $[mim][Tf_2N]$, $[bmmim][Tf_2N] > [apmim][Tf_2N] > [bmim][Tf_2N]$. This trend is in approximate agreement with other dynamic results in this study and *ab initio* calculations in an earlier study.[24] For $[apmim][Tf_2N]$, participation of $-N_{H_2}$ in the cation–anion and cation–cation interactions is believed to be responsible for its higher viscosity compared to $[bmim][Tf_2N]$. The viscosity of ILs is known to increase with C2 (C_R) methylation.[38,63−65] On the basis of recent reports in literature, two main factors, the "entropy hypothesis"[64] and the "defect hypothesis"[65] are needed to explain the changes in the viscosity and other physicochemical properties upon C2 methylation of imidazolium-based ILs.

3.3. Microscopic Structure: Polar and Nonpolar Domains. The first insight about polar and nonpolar domains of ions in ILs can be obtained by an electrostatic potential map (ESP) which is a powerful tool to visualize the three-dimensional charge distribution of molecules that can be obtained using *ab initio* calculations.[6,66] It can be seen in Figure 8 that the atoms of the imidazolium ring (e.g., N_A, C_R, and C_w)

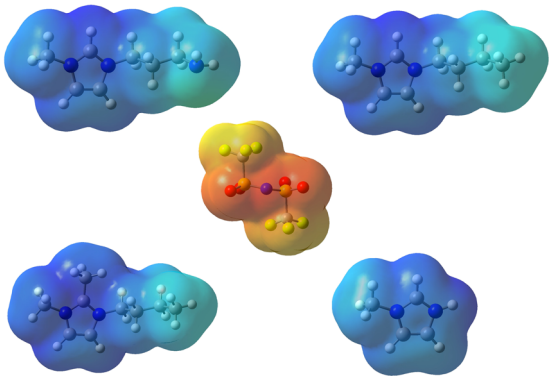

Figure 8. Electrostatic potential map (ESP) or molecular electrical potential surfaces around the studied ions computed using *ab initio* calculation at the B3LYP/6-311++G(d,p) level. The same type of color coding is used in each ion (red color = electron rich and blue color = electron poor).

and hydrogen atom that are directly linked to C_R and C_w (e.g., H_{CR} and H_{CW}) carry most of the positive charge in the cations. The ESP results show the negative charge in anion is distributed mostly on the oxygen and nitrogen atoms. These results can be used in presenting the accumulation of polar and nonpolar domains in these ILs with different coloring code.

The green–red scheme is a very suitable way to demonstrate aggregation and segregation of polar and nonpolar domains in ILs.[6,12,66] In Figure 9, the polar domains are shown in red and include the entire $[Tf_2N]^-$, imidazolium ring, and the hydrogen atoms directly attached to imidazolium ring (H_{CR} and H_{CW}). The nonpolar domains are shown in green and include alkyl-side chains of the imidazolium cation. The snapshot of equilibrated simulation boxes of the studied ILs at 400 K are shown in Figure 9. According to Figure 9, with an increase in alkyl-side chain, aggregation of the alky-side chain in nonpolar

DOI: 10.1021/je500618w
J. Chem. Eng. Data XXXX, XXX, XXX–XXX

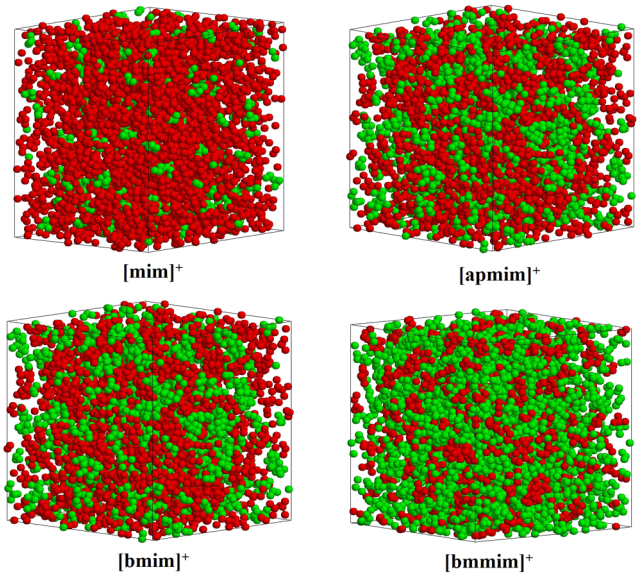

Figure 9. Green−red coloring code snapshots of equilibrated simulation boxes of four ionic liquids in this work, in which polar domains contain whole atoms of $[Tf_2N]^-$; imidazolium ring and directly linked hydrogen atoms (H_{CR}, H_{CW}) were colored in red. In [apmim][Tf_2N] ionic liquid the $-NH_2$ functional group was also colored in red as polar domains. Alkyl-side chains were colored green as nonpolar domains.

domains was observed. For this reason [bmmim][Tf_2N] has the most aggregation of nonpolar domains and segregation between polar and nonpolar parts.

4. SUMMARY AND CONCLUSIONS

The simulation results in this study, which use a nonpolarizable force field, generally tend to underestimate the self-diffusivity and conductivity and overestimate the shear viscosity of ILs. The first and second zero time values in the decay of the ionic VACFs plots occur at longer times with increasing ionic mass, and the heavy $[Tf_2N]^-$ anions have the longest ionic zero time decay scales. The MSD plots show that the motion of the carbon atoms close to the end of the alkyl chains of the imidazolium cations is substantially greater than the motion of the ring atoms (N_A, C_w, C_R) of the imidazolium cation. The order of MSD values at the same times for imidazolium cations is $[bmim]^+ \geq [apmim]^+ > [bmmim]^+ > [mim]^+$, and a similar trend holds for the MSD values of $[Tf_2N]^-$ counterions in the corresponding ILs. The C2 methylation of $[bmim]^+$, or amine ($-NH_2$) functionalization of the end of *n*-butyl side chain of this cation decreases the translation motion and MSDs in [bmmim][Tf_2N] and [apmim][Tf_2N] ILs. The lowest MSD values of both cation and anion are observed in [mim][Tf_2N] which is related to better packing of the ions in the liquid phase, relatively lower intrinsic charge delocalization in $[mim]^+$, and consequently stronger ion association in [mim][Tf_2N] ionic liquid. The calculated electrostatic interaction energies demonstrate [mim][Tf_2N] has greater electrostatic interaction energy than [bmmim][Tf_2N] and [bmim][Tf_2N] ILs. Electrostatic and vdW interaction energies values show electrostatic interactions have a greater contribution in intermolecular energies than vdW interactions in the current ILs. Therefore, [mim][Tf_2N] demonstrated more cation−anion interaction than [bmmim][Tf_2N] and [bmim][Tf_2N] ILs. The observed trend in the intermolecular energies from simulations for these class of ILs is [apmim][Tf_2N] > [mim][Tf_2N] > [bmmim][Tf_2N] > [bmim][Tf_2N].

The trend for ionic conductivity is σ[bmim][Tf_2N] > σ[apmim][Tf_2N] > σ[mim][Tf_2N] > σ[bmmim][Tf_2N]. The [apmim][Tf_2N] ionic liquid with the polar $-NH_2$ functional group in the side chain of imidazolium cation has less ionic conductivity than the [bmim][Tf_2N] ionic liquid. The C2 methylated ionic liquid, [bmmim][Tf_2N], has the lowest ionic conductivity in agreement with high viscosity and slow dynamics observed for C2 methylated ILs. By computing the Green−Kubo ionic conductivity, a deviation from the Nernst−Einstein conductivity behavior was observed and attributed to the degree of the ionic association between cations and anions. In addition, snapshots of equilibrated simulation boxes of ionic liquids in the present study show that [bmmim][Tf_2N] ionic liquid has the most aggregation of nonpolar domains and segregation between polar and nonpolar parts. The opposite of this trend was observed for [mim][Tf_2N].

AUTHOR INFORMATION

Corresponding Author

*E-mail: mhkowsari@iasbs.ac.ir. Tel.: +98 24 3315 3207. Fax: +98 24 3315 3232.

Present Address

[§]M.F.: Department of Chemistry, Sharif University of Technology, Tehran 11365−11155, Iran.

Funding

Support for this work by the Department of Chemistry of the Institute for Advanced Studies in Basic Sciences (IASBS) is gratefully acknowledged. M.H.K. also acknowledges support from the Center for Research in Climate Change and Global Warming (CRCC) in IASBS.

Notes

The authors declare no competing financial interest.

REFERENCES

(1) Cadena, C.; Zhao, Q.; Snurr, R. Q.; Maginn, E. J. Molecular Modeling and Experimental Studies of the Thermodynamic and Transport Properties of Pyridinium-Based Ionic Liquids. *J. Phys. Chem. B* **2006**, *110*, 2821−2832.

(2) Gardas, R. L.; Freire, M. G.; Fonseca, I. M. A.; Ferreira, A. G. M.; Coutinho, J. A. P.; Carvalho, P. J.; Marrucho, I. M. *PρT* Measurements of Imidazolium-Based Ionic Liquids. *J. Chem. Eng. Data* **2007**, *52*, 1881−1888.

(3) Crosthwaite, J. M.; Muldoon, M. J.; Aki, S. N. V. K.; Maginn, E. J.; Brennecke, J. F. Liquid Phase Behavior of Ionic Liquids with Alcohols: Experimental Studies and Modeling. *J. Phys. Chem. B* **2006**, *110*, 9354−9361.

(4) Cadena, C.; Maginn, E. J. Molecular Simulation Study of Some Thermophysical and Transport Properties of Triazolium-Based Ionic Liquids. *J. Phys. Chem. B* **2006**, *110*, 18026−18039.

(5) Dong, K.; Song, Y.; Liu, X.; Cheng, W.; Yao, X.; Zhang, S. Understanding Structures and Hydrogen Bonds of Ionic Liquids at the Electronic Level. *J. Phys. Chem. B* **2012**, *116* (3), 1007−1017.

(6) Pádua, A. A. H.; Gomes, M. F. C.; Lopes, J. N. A. C. Molecular Solutes in Ionic Liquids: A Structural Perspective. *Acc. Chem. Res.* **2007**, *40*, 1087−1096.

(7) Dyson, P. J.; Geldbach, T. J.; *Metal Catalysed Reactions in Ionic Liquids*; Springer: New York, 2006.

(8) Wasserscheid, P., Welton, T., Eds. *Ionic Liquids in Synthesis*; Wiley VCH: Weinheim, Germany, 2002.

(9) Marsh, K. N.; Boxall, J. A.; Lichtenthaler, R. Room Temperature Ionic Liquids and Their Mixtures—A Review. *Fluid Phase Equilib.* **2004**, *219*, 93−98.

DOI: 10.1021/je500618w
J. Chem. Eng. Data XXXX, XXX, XXX−XXX

(10) Dai, S.; Ju, Y. H.; Barnes, C. E. Solvent Extraction of Strontium Nitrate by a Crown Ether Using Room-Temperature Ionic Liquids. *J. Chem. Soc., Dalton Trans.* **1999**, 1201−1202.
(11) Visser, A.; Swatloski, R.; Reichert, W.; Mayton, R.; Sheff, S.; Wierzbicki, A.; Davis, J.; Rogers, R. Task-Specific Ionic Liquids for the Extraction of Metal Ions from Aqueous Solutions. *Chem. Commun.* **2001**, 135−136.
(12) Lopes, J. N. C.; Gomes, M. F. C.; Padua, A. A. H. Nonpolar, Polar, and Associating Solutes in Ionic Liquids. *J. Phys. Chem. B* **2006**, *110*, 16816−16818.
(13) Anthony, J. L.; Maginn, E. J.; Brennecke, J. F. Solution Thermodynamics of Imidazolium-Based Ionic Liquids and Water. *J. Phys. Chem. B* **2001**, *105*, 10942−10949.
(14) Kelkar, M. S.; Maginn, E. J. Effect of Temperature and Water Content on the Shear Viscosity of the Ionic Liquid 1-Ethyl-3-methylimidazolium Bis(trifluoromethanesulfonyl)imide as Studied by Atomistic Simulations. *J. Phys. Chem. B* **2007**, *111*, 4867−4876.
(15) Menjoge, A.; Dixon, J.; Brennecke, J. F.; Maginn, E. J.; Vasenkov, S. Influence of Water on Diffusion in Imidazolium-Based Ionic Liquids: A Pulsed Field Gradient NMR Study. *J. Phys. Chem. B* **2009**, *113*, 6353−6359.
(16) Kowsari, M. H.; Alavi, S.; Najafi, B.; Gholizadeh, K.; Dehghanpisheh, E.; Ranjbar, F. Molecular Dynamics Simulations of the Structure and Transport Properties of Tetra-butylphosphonium Amino Acid Ionic Liquids. *Phys. Chem. Chem. Phys.* **2011**, *13*, 8826−8837.
(17) Holbrey, J. D.; Reichert, W. M.; Rogers, R. D. Crystal Structures of Imidazolium bis(trifluoromethanesulfonyl)imide 'Ionic Liquid' Salts: The First Organic Salt with a cis-TFSI Anion Conformation. *Dalton Trans.* **2004**, 2267−2271.
(18) Zhang, S.; Zhou, G.; Liu, X.; Chen, X. Structure, Interaction and Property of Amino-Functionalized Imidazolium ILs by Molecular Dynamics Simulation and Ab Initio Calculation. *AIChE J.* **2007**, *53*, 3210−3221.
(19) Gutowski, K. E.; Maginn, E. J. Amine-Functionalized Task-Specific Ionic Liquids: A Mechanistic Explanation for the Dramatic Increase in Viscosity upon Complexation with CO_2 from Molecular Simulation. *J. Am. Chem. Soc.* **2008**, *130*, 14690−14704.
(20) Liu, X.; Zhou, G.; Zhang, S.; Yao, X. Molecular Dynamics Simulation of Dual Amino-Functionalized Imidazolium-Based Ionic Liquids. *Fluid Phase Equilib.* **2009**, *284*, 44−49.
(21) Lopes, J. N. C.; Deschamps, J.; Pádua, A. A. H. Modeling Ionic Liquids Using a Systematic All-Atom Force Field. *J. Phys. Chem. B* **2004**, *108*, 2038−2047.
(22) Lopes, J. N. C.; Pádua, A. A. H. Molecular Force Field for Ionic Liquids Composed of Triflate or Bistriflylimide Anions. *J. Phys. Chem. B* **2004**, *108*, 16893−16898.
(23) Lopes, J. N. C.; Pádua, A. A. H.; Shimizu, K. Molecular Force Field for Ionic Liquids IV: Trialkylimidazolium and Alkoxycarbonyl-Imidazolium Cations; Alkylsulfonate and Alkylsulfate Anions. *J. Phys. Chem. B* **2008**, *112*, 5039−5046.
(24) Kowsari, M. H.; Fakhraee, M.; Alavi, S.; Najafi, B. Molecular Dynamics and *ab Initio* Studies of the Effects of Substituent Groups on the Thermodynamic Properties and Structure of Four Selected Imidazolium-Based $[Tf_2N^-]$ Ionic Liquids. *J. Chem. Eng. Data* **2014**, *59*, 2834−2849.
(25) Smith, W.; Forester, T. R.; Todorov, I. T. *The DL_POLY Molecular Simulation Package*, v. 2.18; Daresbury Laboratory: UK, 2007.
(26) Nosé, S. A Unified Formulation of the Constant Temperature Molecular-Dynamics Methods. *J. Chem. Phys.* **1984**, *81*, 511−519.
(27) Melchionna, S.; Ciccotti, G.; Holian, B. L. Hoover *NPT* Dynamics for Systems Varying in Shape and Size. *Mol. Phys.* **1993**, *78*, 533−544.
(28) Hansen, J. P.; McDonald, I. R. *Theory of Simple Liquids*; Academic Press: New York, 1986.
(29) Galiński, M.; Lewandowski, A.; Stępniak, I. Ionic liquids as Electrolytes. *Electrochim. Acta* **2006**, *51*, 5567−5580.
(30) Zhong, X.; Liu, Z.; Cao, D. Improved Classical United-Atom Force Field for Imidazolium-Based Ionic Liquids: Tetrafluoroborate, Hexafluorophosphate, Methylsulfate, Trifluoromethylsulfonate, Acetate, Trifluoroacetate, and Bis(trifluoromethylsulfonyl)amide. *J. Phys. Chem. B* **2011**, *115*, 10027−10040.
(31) Gabl, S.; Schröder, C.; Steinhauser, O. Computational Studies of Ionic Liquids: Size Does Matter and Time Too. *J. Chem. Phys.* **2012**, *137*, 094501.
(32) Tsuzuki, S.; Matsumoto, H.; Shinoda, W.; Mikami, M. Effects of Conformational Flexibility of Alkyl Chains of Cations on Diffusion of Ions in Ionic Liquids. *Phys. Chem. Chem. Phys.* **2011**, *13*, 5987−5993.
(33) Liu, H.; Maginn, E. J. A Molecular Dynamics Investigation of the Structural and Dynamic Properties of the Ionic Liquid 1-*n*-butyl-3-methylimidazolium bis(trifluoromethanesulfonyl)imide. *J. Chem. Phys.* **2011**, *135*, 124507.
(34) Tokuda, H.; Hayamizu, K.; Ishii, K.; Susan, M. A. B. H.; Watanabe, M. Physicochemical Properties and Structures of Room Temperature Ionic Liquids. 1. Variation of Anionic Species. *J. Phys. Chem. B* **2004**, *108*, 16593−16600.
(35) Tokuda, H.; Hayamizu, K.; Ishii, K.; Susan, M. A. B. H.; Watanabe, M. Physicochemical Properties and Structures of Room Temperature Ionic Liquids. 2. Variation of Alkyl Chain Length in Imidazolium Cation. *J. Phys. Chem. B* **2005**, *109*, 6103−6110.
(36) Prado, E. R.; Freitas, L. C. G. Molecular Dynamics Simulation of The Room-Temperature Ionic Liquid 1-Butyl-3-methylimidazolium Tetrafluoroborate. *J. Mol. Struct.: THEOCHEM* **2007**, *847*, 93−100.
(37) Kowsari, M. H.; Alavi, S.; Ashrafizaadeh, M.; Najafi, B. Molecular Dynamics Simulation of Imidazolium-Based Ionic Liquids. I. Dynamics and Diffusion Coefficient. *J. Chem. Phys.* **2008**, *129*, 224508.
(38) Liu, H.; Maginn, E. J.; Visser, A. E.; Bridges, N. J.; Fox, E. B. Thermal and Transport Properties of Six Ionic Liquids: An Experimental and Molecular Dynamics Study. *Ind. Eng. Chem. Res.* **2012**, *51*, 7242−7254.
(39) Rey-Castro, C.; Vega, L. F. Transport Properties of the Ionic Liquid 1-Ethyl-3-methylimidazolium Chloride from Equilibrium Molecular Dynamics Simulation. The Effect of Temperature. *J. Phys. Chem. B* **2006**, *110*, 14426−14435.
(40) Androulaki, E.; Vergadou, N.; Ramos, J.; Economou, I. G. Microscopic Structure of Ionic Liquids Based on Molecular Dynamics Simulation. *Mol. Phys.* **2012**, *110*, 1139−1152.
(41) Zhao, W.; Leroy, F.; Heggen, B.; Zahn, S.; Kirchner, B.; Balasubramanian, S.; Müller-Plathe, F. Are There Stable Ion-Pairs in Room-Temperature Ionic Liquids? Molecular Dynamics Simulations of 1-*n*-Butyl-3-methylimidazolium Hexafluorophosphate. *J. Am. Chem. Soc.* **2009**, *131*, 15825−15833.
(42) Bedrov, D.; Borodin, O.; Li, Z.; Smith, G. D. Influence of Polarization on Structural, Thermodynamic, and Dynamic Properties of Ionic Liquids Obtained from Molecular Dynamics Simulations. *J. Phys. Chem. B* **2010**, *114*, 4984−4997.
(43) Borodin, O. Polarizable Force Field Development and Molecular Dynamics Simulations of Ionic Liquids. *J. Phys. Chem. B* **2009**, *113*, 11463−11478.
(44) Andreussi, O.; Marzari, N. Transport Properties of Room Temperature Ionic Liquids from Classical Molecular Dynamics. *J. Chem. Phys.* **2012**, *137*, 044508.
(45) Lee, S. U.; Jung, J.; Han, Y. K. Molecular Dynamics Study of the Ionic Conductivity of Ionic Liquids 1-n-Butyl-3-methylimidazolium Salts. *Chem. Phys. Lett.* **2005**, *406*, 332−340.
(46) Rey-Castro, C.; Tormo, A. L.; Vega, L. F. Effect of the Flexibility and the Anion in the Structural and Transport Properties of Ethyl-methyl-imidazolium Ionic Liquids. *Fluid Phase Equilib.* **2007**, *256*, 62−69.
(47) Kowsari, M. H.; Alavi, S.; Ashrafizaadeh, M.; Najafi, B. Molecular Dynamics Simulation of Imidazolium-Based Ionic Liquids. II. Transport Coefficients. *J. Chem. Phys.* **2009**, *130*, 014703.
(48) Liu, H.; Maginn, E. J. An MD Study of the Applicability of the Walden Rule and the Nernst−Einstein Model for Ionic Liquids. *ChemPhysChem* **2012**, *13*, 1701−1707.

DOI: 10.1021/je500618w
J. Chem. Eng. Data XXXX, XXX, XXX−XXX

(49) Kashyap, H. K.; Annapureddy, H. V. R.; Raineri, F. O.; Margulis, C. J. How Is Charge Transport Different in Ionic Liquids and Electrolyte Solutions? *J. Phys. Chem. B* **2011**, *115*, 13212−13221.
(50) Harris, K. R. Relations between the Fractional Stokes−Einstein and Nernst−Einstein Equations and Velocity Correlation Coefficients in Ionic Liquids and Molten Salts. *J. Phys. Chem. B* **2010**, *114*, 9572−9577.
(51) Del Pópolo, M. G.; Voth, G. A. On the Structure and Dynamics of Ionic Liquids. *J. Phys. Chem. B* **2004**, *108*, 1744−1752.
(52) Bonhôte, P.; Dias, A.; Papageorgiou, P. N.; Kalyanasundaram, K.; Grätzel, M. Hydrophobic, Highly Conductive Ambient-Temperature Molten Salts. *Inorg. Chem.* **1996**, *35*, 1168−1178.
(53) Noack, K.; Schulz, P. S.; Paape, N.; Kiefer, J.; Wasserscheid, P.; Leipertz, A. The Role of the C2 Position in Interionic Interactions of Imidazolium Based Ionic Liquids: A Vibrational and NMR Spectroscopic Study. *Phys. Chem. Chem. Phys.* **2010**, *12*, 14153−14161.
(54) Malham, I. B.; Turmine, M. Viscosities and Refractive Indices of Binary Mixtures of 1-Butyl-3-methylimidazolium Tetrafluoroborate and 1-Butyl-2,3-dimethylimidazolium Tetrafluoroborate with Water at 298 K. *J. Chem. Thermodyn.* **2008**, *40*, 718−723.
(55) Podgorŝek, A.; Salas, G.; Campbell, P. S.; Santini, C. C.; Pádua, A. A. H.; Gomes, M. F. C.; Fenet, B.; Chauvin, Y. Influence of Ionic Association, Transport Properties, and Solvation on the Catalytic Hydrogenation of 1,3-Cyclohexadiene in Ionic Liquids. *J. Phys. Chem. B* **2011**, *115*, 12150−12159.
(56) MacFarlane, D. R.; Forsyth, M.; Izgorodina, E. I.; Abbott, A. P.; Annat, G.; Fraser, K. On the Concept of Ionicity in Ionic Liquids. *Phys. Chem. Chem. Phys.* **2009**, *11*, 4962−4967.
(57) Ueno, K.; Tokuda, H.; Watanabe, M. Ionicity in Ionic Liquids: Correlation with Ionic Structure and Physicochemical Properties. *Phys. Chem. Chem. Phys.* **2010**, *12*, 1649−1658.
(58) Ue, M.; Murakami, A.; Nakamura, S. A Convenient Method to Estimate Ion Size for Electrolyte Materials Design. *J. Electrochem. Soc.* **2002**, *149*, A1385−A1388.
(59) Voronel, A.; Veliyulin, E.; Machavariani, V. Sh.; Kisliuk, A.; Quitmann, D. Fractional Stokes−Einstein Law for Ionic Transport in Liquids. *Phys. Rev. Lett.* **1998**, *80*, 2630−2633.
(60) Harris, K. R.; Kanakubo, M.; Tsuchihashi, N.; Ibuki, K.; Ueno, M. Effect of Pressure on the Transport Properties of Ionic Liquids: 1-Alkyl-3-methylimidazolium Salts. *J. Phys. Chem. B* **2008**, *112*, 9830−9840.
(61) Spohr, H. V.; Patey, G. N. Structural and Dynamical Properties of Ionic Liquids: The Influence of Ion Size Disparity. *J. Chem. Phys.* **2008**, *129*, 064517.
(62) Köddermann, T.; Ludwig, R.; Paschek, D. On the Validity of Stokes−Einstein and Stokes−Einstein−Debye Relations in Ionic Liquids and Ionic-Liquid Mixtures. *ChemPhysChem* **2008**, *9*, 1851−1858.
(63) Endo, T.; Imanari, M.; Seki, H.; Nishikawa, K. Effects of Methylation at Position 2 of Cation Ring on Rotational Dynamics of Imidazolium-Based Ionic Liquids Investigated by NMR Spectroscopy: [C_4mim]Br vs. [C_4C_1mim]Br. *J. Phys. Chem. A* **2011**, *115*, 2999−3005.
(64) Hunt, P. A. Why Does a Reduction in Hydrogen Bonding Lead to an Increase in Viscosity for the 1-Butyl-2,3-dimethyl-imidazolium Based Ionic Liquids? *J. Phys. Chem. B* **2007**, *111*, 4844−4853.
(65) Fumino, K.; Wulf, A.; Ludwig, R. Strong, Localized, and Directional Hydrogen Bonds Fluidize Ionic Liquids. *Angew. Chem., Int. Ed.* **2008**, *47*, 8731−8734.
(66) Shimizu, K.; Gomes, M. F. C.; Pádua, A. A. H.; Rebelo, L. P. N.; Lopes, J. N. C. Three Commentaries on the Nano-segregated Structure of Ionic Liquids. *J. Mol. Struct.: THEOCHEM* **2010**, *946*, 70−76.

DOI: 10.1021/je500618w
J. Chem. Eng. Data XXXX, XXX, XXX−XXX